Spiking Oscillations in Complex Neuronal Networks

Luciano da Fontoura Costa
Institute of Physics at São Carlos, University of São Paulo, P.O. Box 369, São Carlos, São Paulo, 13560-970 Brazil (Copyright Luciano da F. Costa, 2008)
(Dated: 10th Feb 2008)

Although integrate-and-fire dynamics possesses special importance because of its intrinsic relationship with neuronal information processing, it has been rarely considered in investigations of the structure-dynamics relationship in complex networks. However, the pronounced non-linearities of this type of dynamics implies a particularly rich variety of attractors and activity patterns, including avalanches of spikes and confinement of activation inside topological communities. Both these remarkable phenomena take place during the transient activation regime. In this work we investigate the oscillations and waves which appear in the equilibrium regime of integrate-and-fire complex neuronal networks. In order to do so, one of the restrictions of the equivalent models reported previously, namely a reasonable uniformity of degrees, is circumvented by subsuming the nodes with identical degree found inside each hierarchical levels into respective equivalent nodes. It has been shown, by considering uniformly-random and small-world theoretical types of networks, that the so-obtained model is capable of predicting the respective integrate-and-fire dynamics with great accuracy regarding both temporal dynamics and power spectrum features. The causes and properties of the stable waves emerging along the equilibrium regime of the complex neuronal networks are identified and discussed. Of particular relevance are the twin correlations defined by the different frequencies of groups of nodes at different concentric levels. The transient and equilibrium regimes are also clearly identifiable from the total activation in the networks, corresponding respectively to conservative and dissipative dynamics.

PACS numbers: 87.18.Sn, 89.75.Hc, 87.18.Fx, 89.45.+i, 89.75.Fb, 89.75.-k

'Andria was built so artfully that its every street follows a planet's orbit, and the buildings and the places of community life repeat the order of the constellations and the position of the most luminous stars...' (Invisible Cities, I. Calvino)

I. INTRODUCTION

Despite the great current interest in the structure and dynamics relationship in complex networks (e.g. [1–12], very few works have been reported addressing the non-linear dynamics implied by the integrate-and-fire model of neuronal cells. This type of non-linear dynamics is particularly important because it is intrinsically associated to the workings of nervous systems (e.g. [13–15]), being critically related to memory as well as the important cognitive tasks of control and pattern recognition, which seem to be essentially dependent of non-linear dynamics features and not obtainable by linear activations. In addition, several other real-world situations can be effectively modeled by the integrate-and-fire model, including transportation systems, information processing, disease spreading, and gene expression, amongst many other important complex systems.

The rich variety of dynamics allowed by the integrate-and-fire model when underlain by complex networks has been corroborated in a recent series of works ([16–20]) and includes the identification of avalanches of spikes [16] and activation confinement within the network communities [17, 18] during the transient regime of integrate-and-fire complex neuronal networks. These two phenomena have been effectively modeled and explained by using equivalent models of the complex neuronal networks ([19, 20]) which take into account the hierarchical organization of the respective connectivity. Another interesting feature induced by integrate-and-fire dynamics on complex networks are the oscillations of the number of spikes, identified in [19] and preliminary illustrated in [20], which corresponds to the main subject of the present work.

The first equivalent model, reported in [19], was obtained by taking into account the *hierarchical structure* of complex networks (e.g. [21–24]), more specifically the *hierarchical number of nodes* and *hierarchical degrees*. While assuming a reasonable uniformity of degrees amongst the nodes at each level, a *chain equivalent model* was suggested where all nodes at each concentric level are subsumed [25] into an equivalent node. This approach allowed predictions of the intensity and timing of the main avalanches of spikes during the transient neuronal activation [19]. This model was subsequently enhanced to incorporate the edges inside each concentric level as well as complex networks with asymmetric connections (i.e. not all directed edges have the respective opposite counterpart) [20]. Such modifications allowed the equivalent model to be extended to represent any integrate-and-fire neuronal network, including *modular complex neuronal networks* [20]. This model provided impressive predictions of the non-linear dynamics in each of the communities within a given modular complex network.

The current article investigates to a greater extension the saw oscillations and waves identified during the transient and equilibrium regimes of integrate-and-fire complex neuronal networks [19, 20]. In a preliminary ap-

proach (unreported), the enhanced equivalent model incorporating intra-ring edges and asymmetric edges [20] was applied in order to obtain insights about the origin of the waves and oscillations while considering several types of connectivity (e.g. Erdős-Rényi, Barabási-Albert, etc.). As in the previous works, the networks were activated from a source node. However, poor results were obtained, suggesting that there were additional important features of the complex networks which were not included in the enhanced in the equivalent model yet. These features ultimately turned out to be, at least partially, deviations from the basic assumption of nearly-uniform node degrees which had been adopted previously. Therefore, one of the remaining limitations of the equivalent models had to be addressed and overcome, which was done by subsuming into additional equivalent nodes all the nodes within each level which had identical degrees. Thus, instead of mapping a whole concentric level into an equivalent node, as done in [19], each of such levels was partitioned into two or more equivalent nodes associated to the nodes in each hierarchical level which had identical degrees.

The so-obtained enhanced equivalent model, reported in this work, allowed impressively accurate predictions of the transient and equilibrium integrate-and-fire dynamics in several theoretical types of networks, allowing not only the identification and characterization of the oscillations and waves at the equilibrium regime, but also motivating the definition of new hierarchical measurements related to the degree distribution within each concentric level.

This article starts by briefly reviewing the basic concepts required for the understanding of the herein reported developments and proceeds by describing the new equivalent model, accounting for non-uniform degree distributions, and its application to the prediction of the oscillatory dynamics in two types (uniformly-random and small-world models) of integrate-and-fire complex neuronal networks. Though additional types of networks have been also investigated, the latter type provides a specially interesting case because of its several concentric levels. Both these networks yielded a relatively large dispersion of node degrees. The so-obtained insights were then discussed with respect to the several types of characterizations and obtained results. The article concludes by identifying its main contributions and the respective prospects for further developments.

II. BASIC CONCEPTS

A. Complex Networks Representation and Characterization

A directed, weighted complex network can be represented in terms of its *weight matrix* W, so that $W(j,i)$ represents the weight of the edge extending from node i to node j. The respective *adjacency matrix* K can be obtained by transforming into 1 all non-zero weights. The *immediate neighbors* of a node i are those nodes which receive an edge from i. The *out-degree* of a node i is equal to the number of its immediate neighbors. Two edges are *adjacent* if they share a node. Two nodes are adjacent whenever they share an edge. A sequence of adjacent edges define a *walk*. A path is a walk which never repeats nodes or edges. The *length* of a path (or walk) is equal to the number of edge it contains.

B. Hierarchical Organization of Complex Networks

Given a complex network and a *reference node* i, its *hierarchical organization* can be obtained by flooding the network from the reference node [21]. The hierarchical organization includes the *concentric levels* (or hierarchical levels) of the network, namely the levels containing the nodes which are at successive shortest path distances from the reference node i. So, the first concentric level incorporates the original nodes which are at shortest path distance 1 from i (i.e. they are the immediate neighbors of i). The second concentric level includes the nodes which are at shortest path distance 2 from i, and so on. The connections between the reference node and the nodes at the $h-$level can be understood as implementing *virtual links* [26]. Once the hierarchical organization of a network has been obtained with respect to a specific node chosen as the reference, a series of measurements can be calculated [21–24], including the *hierarchical number of nodes* $n_h(i)$, the *hierarchical degree* $k_h(i)$ and the *intra-ring degree* $a_h(i)$. The hierarchical number of nodes corresponds to the number of nodes within each respective concentric level. The hierarchical degree is equal to the number of edges from level h to level $h+1$. The intra-ring (or intra-level) degree corresponds to the number of edges established within level h.

With the extension of the hierarchical organization to complex networks with asymmetric connections [20], the hierarchical degree needs to be split into *hierarchical indegree* and *hierarchical outdegree*. Therefore, the hierarchical indegree of level h with respect to node i, henceforth abbreviated as $ki_h(i)$, is equal to the number of edges received by level h from level $h-1$. The hierarchical outdegree of level h is the number of edges sent from that level to level $h+1$.

C. Theoretical Models of Complex Networks

Two types of complex networks are considered in this work: the uniformly-random network Erdős-Rényi (ER) network [35]) and Watts-Strogatz small-world structures (WS). The ER networks are obtained by assigning edges between pairs of nodes with fixed probability. The Watts-Strogatz networks adopted in this work start as linear lattices with proper number of adjacent connections, with subsequent rewiring of 10% of the edges. Only the largest connected components of each of these 2 models are con-

sidered in this work. Directed complex neuronal networks are respectively obtained by splitting each of the undirected edges into two directed edges with opposite directions (henceforth called asymmetric directed connections).

D. Integrate-and-Fire Model

The integrate-and-fire neuron adopted in the present work is shown in Figure 1. It includes three components: (i) integrator Σ, (ii) memory $S(i)$ storing the accumulated activation; and (iii) threshold element $T(i)$. Once the activation, received from the dendrites with respective weight modulation and integrated into $S(i)$ (facilitation [13]), reaches the threshold value $T(i)$, the neuron fires, producing a spike which is conveyed by the respective axons to the adjacent neurons. The spike activation is divided among the outgoing edges (axons), so that each axon conveys $1/outdeg$, where $outdeg$ is the out-degree of the firing node. Unlike in previous works [16–20], the activation inside each memory $S(i)$ is limited to $L(i)$ at all times. This implies that the portion of the activation received by a node which exceeds $L(i)$ is discarded, therefore undermining the conservation of the activation received from the source node after the neurons start firing.

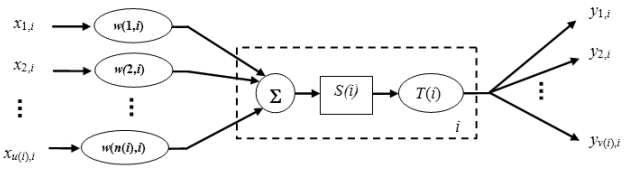

FIG. 1: The integrate-and-fire model of neuronal cell adopted in the present work. It incorporates three components: (i) integrator; (ii) memory (integrated activation) $S(i)$; and (iii) threshold $T(i)$. Once fired, all axons emanating from neuron i will convey the same amount of activation (equal to 1).

Oscillations have also been observed for the more biologically-realistic situation in which the transfer activation is constant (as in the action potential), though they tend to take place along more limited parameter configurations. These configurations will be explored in a forthcoming work.

E. Spectral Characterization

Given a time series or signal $s(t)$, it is often quite difficult to identify its periodical components. By reinforcing the intrinsic periodicities along the signal, its *autocorrelation* allows a more effective means for inferring its constituent oscillations. In this work we resource to the *power spectrum* $P(f)$ of the signal $s(t)$, which corresponds to the squared magnitude of the Fourier transform of the autocorrelation of $s(t)$ [27]. More specifically, given the signal $s(t)$, its Fourier transform is defined as

$$S(f) = \int_{t=-\infty}^{\infty} s(t) exp(-i2\pi ft) dt$$

The autocorrelation of $s(t)$ is

$$a(\tau) = \int_{t=-\infty}^{\infty} s(t)s(\tau - t) dt$$

Therefore, the Fourier transform of the autocorrelation function is immediately given by the correlation theorem as

$$A(f) = S(f)S(f)^*$$

where '$S(f)^*$' is the conjugate of S. The *magnitude of the spectrum* of $s(t)$ is

$$|A(f)| = \sqrt{S(f)S(f)^*} dt$$

The *power spectrum* of $s(t)$ is defined as being equal to the squared magnitude of the spectrum of $s(t)$, i.e.

$$P(f) = S(f)S(f)^*$$

The power spectrum allows the identification of autocorrelations (especially oscillations) of the original signal. More specifically, presence of peaks at specific frequencies f in the power spectrum indicate the presence of respective oscillations with frequency f in the original signal $s(t)$. All power spectra in this work are estimated by using the Fast Fourier Transform (FFT).

F. Multivariate Statistical Methods

The spikes produced along time for each neuron in the complex neuronal networks can be understood as *patterns*, which can be compared and classified by using multivariate statistics [27–29] and/or pattern recognition methods [27, 29]. In the present work, we apply the Principal Component Analysis (PCA) methodology [27, 30] in order to decorrelate the spike patterns [31] and to obtain more significant clusters in respective projections of the original patterns.

Given a set of M spike patterns along H time steps, a total of H measurements corresponding to the presence

of a spike at each time can be obtained. Let us define the matrix U so that each of its rows corresponds to a train of spikes, so that U has dimension $M \times H$. Let $\vec{\mu}$ be the $1 \times H$ vector containing the average number of spikes at each time step $h = 1, 2, \ldots, H$. Now, define the new matrix F as

$$F = U - ones(M, 1)\vec{\mu}$$

where $ones(M, 1)$ is a $M \times 1$ vector of ones. The *covariance matrix*, taking into account all pairwise covariances, is immediately given as

$$C = \frac{1}{M-1} F F^T$$

Observe that C is symmetric. Let λ_i be the eigenvalues of C sorted in descending order, with respective eigenvectors $\vec{v_i}$. The Karhunen-Loève transform of the original measurements is the stochastic linear transformation implemented by the matrix G given as follows

$$G = \begin{bmatrix} \longleftarrow & \vec{v_1} & \longrightarrow \\ \longleftarrow & \vec{v_2} & \longrightarrow \\ \ldots & \ldots & \ldots \\ \longleftarrow & \vec{v_m} & \longrightarrow \end{bmatrix} \quad (1)$$

The PCA method involves transforming the original measurements as $V = GU^T$ with $m << H$, as allowed by the high redundancy normally found along and between signals. It can be shown that the resulting new measurements V, which correspond to linear combinations of the original measurements, are completely decorrelated by the PCA methodology, therefore maximizing the variation of the data long the first new variables.

III. THE EQUIVALENT MODEL FOR NON-UNIFORM DEGREES

Figure 2 illustrates the procedure which had to be adopted in order to obtain the a more effective version of the equivalent model of complex networks, by taking into account non-uniformities of degrees amongst the original nodes. First, the hierarchical organization of the original network with reference to a given node i is obtained (Fig 2). In this specific case we have 5 concentric levels ($h = 0, 1, \ldots, H = 4$), each containing $1, 3, 6, 2$ and 1 nodes (i.e. $n_0(i) = 1$; $n_1(3) = 1$; $n_2(i) = 6$; $n_3(i) = 2$; $n_4(i) = 1$). The nodes within each concentric level which have identical degrees are then subsumed into equivalent nodes. Thus, nodes 3 and 4 at level $h = 1$ — all with degree equal to 5 — become associated to the equivalent node **B**. Nodes 5, 6 and 7, which have degree 4, are subsumed by node **F**. The topology of the resulting equivalent model is illustrated in Figure reffig:equiv.

Now, the weights associated to the edges in the equivalent structure in Figure 2 are determined, similarly as done in [20], by means of the following equation, applied to each pair of equivalent nodes v and p

$$W(v, p) = k(v, p)/d$$

where $k(v, p)$ is the number of original edges going from the nodes associated to the equivalent node p to the nodes associated to the equivalent node v, $d = \sum_{g \in \Omega(p)} k(g, p)$ and $\Omega(p)$ is the set of equivalent nodes that receive a directed edge from p. Obseve that $W(b, a)$ expresses the weight of the connection from a to b. The weights therefore obtained for the graph in Figure 2 are given as follows

$$W = \begin{bmatrix} 0 & 1/5 & 1/3 & 0 & 0 & 0 & 0 \\ 2/3 & 1/5 & 0 & 1/2 & 1/4 & 0 & 0 \\ 1/3 & 0 & 0 & 0 & 1/8 & 0 & 0 \\ 0 & 1/5 & 0 & 0 & 0 & 0 & 0 \\ 0 & 2/5 & 0 & 0 & 1/4 & 4/6 & 0 \\ 0 & 0 & 2/3 & 0 & 3/8 & 1/6 & 1 \\ 0 & 0 & 0 & 1/2 & 0 & 1/6 & 0 \end{bmatrix}$$

For instance, as the two original nodes associated to the equivalent node **B**, both of which with degree 5, send two edges to the equivalent node **A**, two edges to **D**, four edges to **E**, while two edges remain inside **B**, we have $W(A, B) = 1/5$; $W(D, B) = 1/5$; $W(E, B) = 2/5$; $W(B, B) = 1/5$.

The thresholds associated to neuron corresponding to each equivalent node are immediately given as the number of original nodes associated to that equivalent node. Therefore, we have that $T(A) = 1$; $T(B) = 2$; $T(C) = 1$; $T(D) = 2$; $T(E) = 1$; $T(F) = 3$; $T(G) = 2$; and $T(H) = 1$. The limitations to the activations stored into each memory are also set as being equal to the respective number of nodes within each equivalent node, i.e. $T(i) = L(i)$. Observe that the so-obtained equivalent network itself correspond to an integrate-and-fire complex neuronal networks with varying thresholds.

IV. OSCILLATIONS IN UNIFORMLY-RANDOM NETWORKS

In this section we consider a series of complementary approaches in order to characterize the transient and equilibrium dynamics in two types of integrate-and-fire complex neuronal networks — namely ER and WS structure. Representative samples of each of theses types of networks have been selected with sizes $N = 25, 50$ and 100 and average degrees $\langle k \rangle = 10, 20, 30, 40$ and 50.

Figure 3 shows the spikegrams obtained for the several configurations of ER networks. Observe the sell-defined

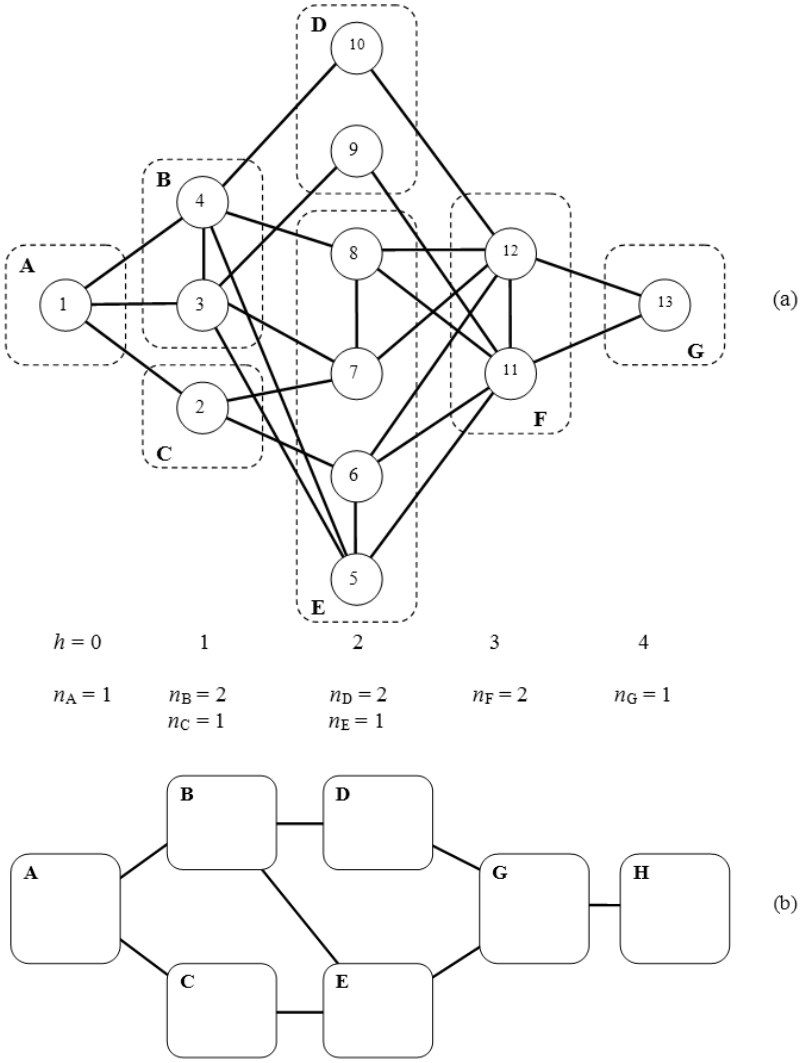

FIG. 2: The hierarchical organization of a simple network (a) with respect to node 1. A total of 5 concentric levels have been obtained. The dotted boxed identify the nodes with identical degrees at each concentric level, which are subsumed by the respective equivalent nodes, yielding the equivalent network shown in (b).

avalanche transitions at the beginning of the spikes obtained for all network configurations. In agreement with previous results [19], the avalanches initiation times were found to be quite similar for all network sizes, irrespectively of the average degree. The early spikes obtained for $N = 50$ and $\langle k \rangle = 10$; $N = 100$ and $\langle k \rangle = 10$; $N = 100$ and $\langle k \rangle = 20$ and $N = 100$; $\langle k \rangle = 30$ and $\langle k \rangle = 50$ were a consequence of the existence of communities which arise in the ER networks arising from random fluctuations. Interestingly, the oscillations tended to become more regular (more similar frequencies) and synchronized with the increase of the average degree. The routes to regularity and synchronization this parameter is increased exhibited groups of neurons producing similar spiking patterns.

The total number of spikes, shown in Figure 4 reflects the ensemble behavior of the respective complex neuronal networks, arising as a consequence of the linear superposition of the spikes being produced by each neuron (analogous to EEG potentials). The avalanche transitions can be clearly identified, taking place after nearly 40 steps for $N = 25$, 40 steps for $N = 50$ and 80 steps for $N = 100$, which confirms the previous study reported in [19]. In several cases, a clear intense peak is observed at the avalanche time, which is followed by oscillations whose regularity tend to increase with the average degree.

In addition to the total number of spikes, it is also important to take into account the respective power spectra, which are shown in Figure 5. Only the second half

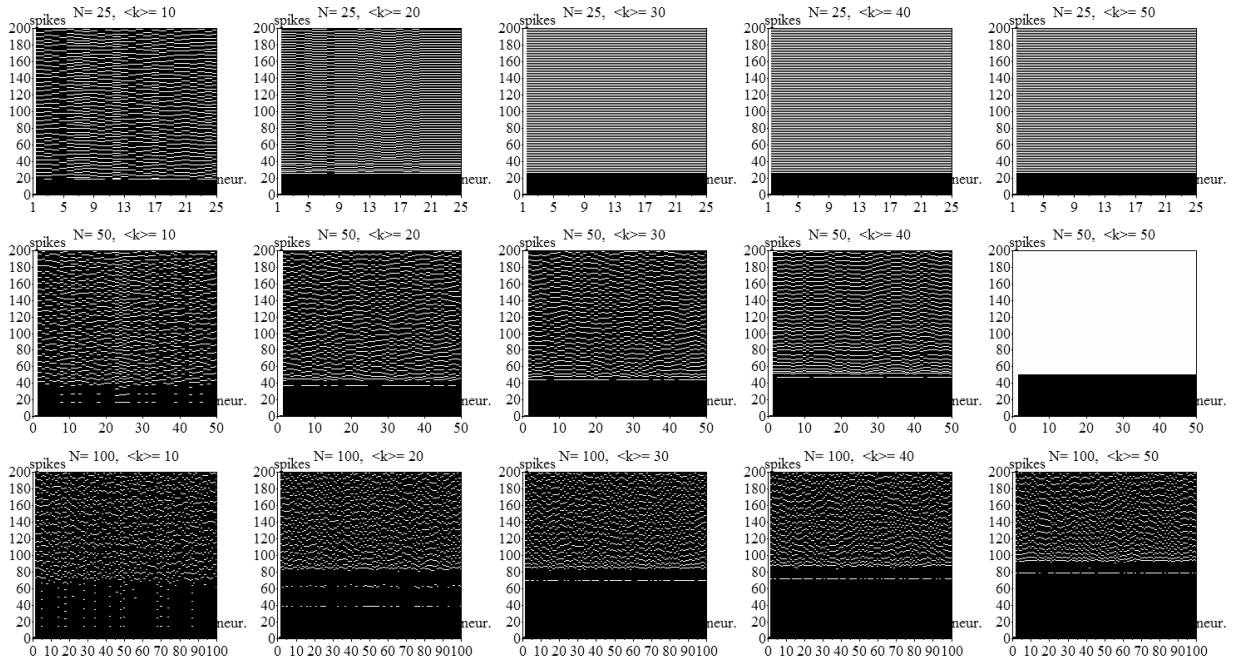

FIG. 3: The spikegrams, i.e. the occurrence of spikes for each neuron (identified along the $x-$axis) along time ($y-$axis) obtained for the ER configurations. Observe the avalanche transitions during the transient regime, as well as the increase of frequency regularity and synchronization with observed for larger values of average degree.

of each signal (number os spikes) has been considered for the calculation of the power spectra in order to represent the equilibrium regime. So, a total $H = 500$ time steps have been considered for the estimation of each spectrum.

Relatively rich spectral composition can be observed for most cases, suggesting particularly complex behavior of the oscillatory components. The progressive elimination of frequencies with the increase of the average degree is evident from Figure 5, especially for $N = 50$ and $N = 100$. In addition, the peaks of the spectra for $N = 50$ and $N = 100$ tend to appear near 20 and 10 frequency units, respectively. At the same time, it should be observed that the peaks of the spectra in Figure 5 tend to shift to the right-hand side for larger values of the average degree, signaling the increase of the main frequencies. The more regular oscillations obtained for larger average degrees are related to the fact that the higher this parameter, the more regular the degrees of the networks become. At the limit, for very large average degree, all nodes become connected, implying a highly regular structure as far as all possible topological features are concerned.

Unlike in the previous works [16–20], the activation inside each neuron is limited to the respective maximum value $L(i)$. In addition to being more biologically-realistic, such a choice also allowed particularly interesting oscillatory dynamics. At the same time, the limitation of the internal activation implies that the overall activation, constantly received from the source node, is no longer guaranteed to be conserved. It is therefore interesting to consider the total activation inside the whole complex neuronal networks along time. Such a measurement is depicted in Figure 6. Interestingly, two clearly distinct regimes are immediately identified: one transient period in which the internal activation increases linearly, followed by the steady-state regime characterized by nearly constant activation (even though activation is continuously pumped into the system through the source node). The transition between these two regimes is in most cases characterized by one abrupt surge of activation, related to the main avalanche. Such a result suggests that the main avalanche represents watershed *signaling the transition of the dynamics in the system from conservative to dissipative*.

Because the train of spikes produced by each individual neuron, shown in Figure 3, seems to be organized in clusters during the route towards more regular and synchronous firing (i.e. similar trains of spikes are obtained for groups of neurons), it is interesting to investigate such a possibility further. We do this with the help of the PCA method, which produced the results shown in Figure 7.

It is clear from this figure that the increase of the average node degree tends to produce denser groups of spiking patterns. At the same time, interesting clustering structures are obtained for small average node degrees, incorporating a dense central cluster (e.g. the PCA scatterplots for $N = 25$ and $\langle k \rangle = 10$, $N = 50$ and $\langle k \rangle = 10$, and $N = 100$ and $\langle k \rangle = 10$) surrounded by outliers. The

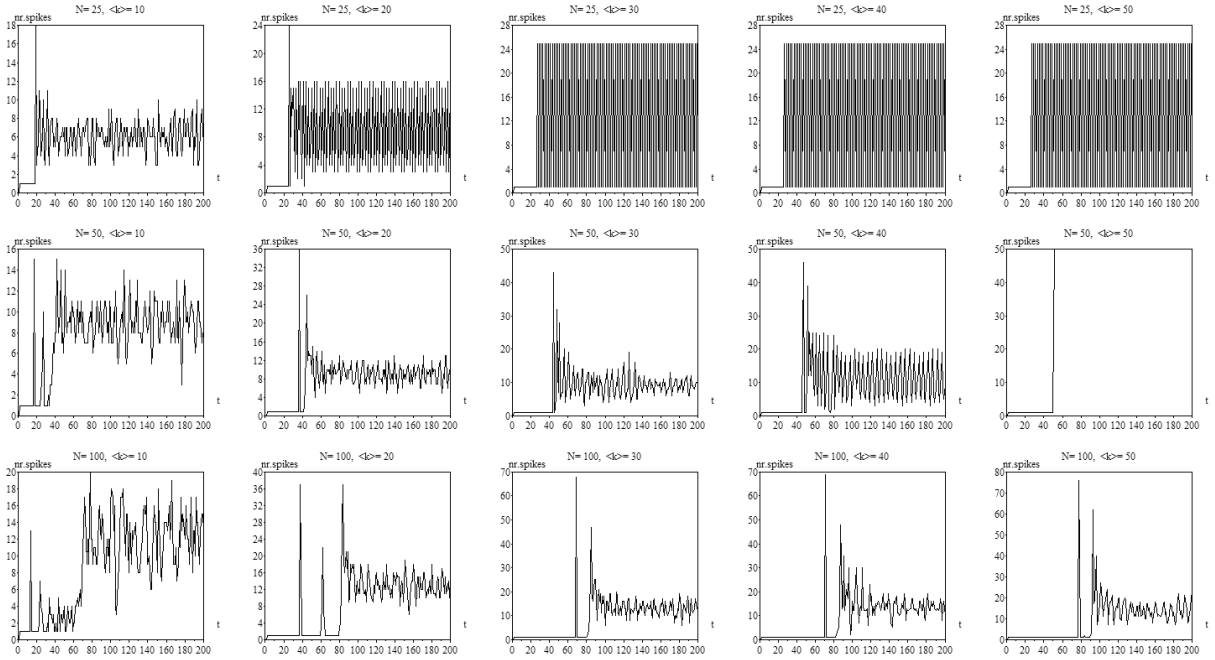

FIG. 4: The number of spikes along time obtained for the original ER complex network configurations.

dense cluster of spiking patterns tend to survive even for relatively large average degrees in the case of $N = 100$.

The correlations between the total number of spikes produced by each neuron during the simulations and the respective degrees have also been considered, yielding some of the most interesting results reported in the present work. These scatterplots are shown in Figure 8. Striking twin-linear correlation patterns have been obtained throughout. Such scatterplots indicate that a node with a given degree can spike at two distinct frequencies of spikes, with the number of spikes being linearly related to the node degrees. At the same time, given one of such rules, the number of spikes (i.e frequency) tends to be correlated with the degree of the original nodes. Such twin correlations are likely to be related to clusters of original nodes appearing at different concentric hierarchical levels, as discussed further in Section VII.

V. OSCILLATIONS IN SMALL-WORLD NETWORKS

Having obtained a comprehensive characterization of the oscillations induced along the equilibrium regime in ER networks, it is interesting to shift our attention to the steady-state dynamics of WS integrate-and-fire activations. Figure 9 shows the spikegrams obtained for the several parametric configurations of the WS models.

Several interesting features are evident from the results shown in Figure 9. Foremost are the more gradual avalanches, which tend to be centralized around the source node (node 1) [36]. Longer avalanche initiation times are implied by larger network sizes N. Because the increase of the average degree implies more degree-regular networks, the gradual activation of the neurons observed for relatively smaller average node degrees became sharper for larger average node degrees. As with the ER cases, the spiking patterns also tended to become more regular and synchronized for larger values of average degree.

Figure 10 depicts the power spectra obtained for each of the considered WS configurations. Such spectra, which were obtained by considering the equilibrium regime of the spikings (i.e. the time steps from 500 to 1000) are remarkably similar to those obtained by the ER structures (Fig. 5, suggesting some possible universality between different complex networks types.

Regarding the total activation inside the system, the revealed results (not shown in this work) also included the two regimes as in the ER case, but with sublinear increase during the transient regime, which was also duly followed by the dissipative plateau of overall activation.

Figure 8 shows the scatterplots of the original node degrees and total number of spikes induced by each individual neuronal cell. Though these two features also tended to be organized in terms of parallel straight groups for small values of average degree, the correlations are now substantially less definite.

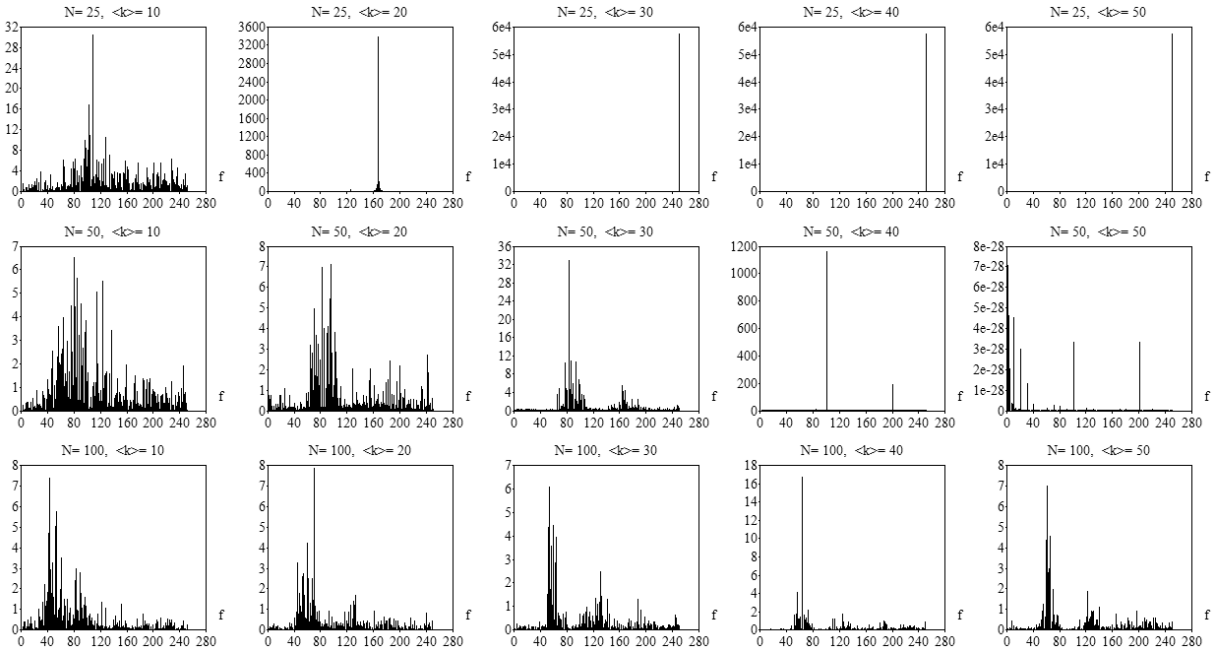

FIG. 5: The power spectra obtained for the number of spikes produced by the whole original ER networks.

VI. EQUIVALENT MODEL PREDICTIONS

Having characterized the oscillatory integrate-and-fire dynamics along the transient and equilibrium regimes in terms of several measurements, it is time to consider the respective equivalent models. The importance of such an approach lies in the fact that these structures involve a fraction of the original number of nodes, therefore allowing the identification and theoretical modeling of more definite relationships between structure and dynamics. We start by considering the distribution of the equivalent nodes and weights, as well as by comparing the predicted and real number of spikes and spectra for ER.

Tables I and II give several features of the topological structure of the equivalent models obtained for each of the ER and WS configurations, respectively. These features include the total number of original nodes in each concentric level (upper line), the hierarchical degrees (second line), the total number of equivalent nodes (in bold, third line), and the number of equivalent nodes per concentric level (within brackets, third line). It is clear from such measurements that the WS structure implied a larger number of concentric levels in all cases. On the other hand, most of the ER structures implied two or three levels (the first of each level corresponding to the source node), except for the network with $N = 100$ and $\langle k \rangle = 10$, which implied 4 concentric levels. Also, because of its greater degree uniformity, the WS model yielded substantially fewer equivalent nodes than the ER structures. The relatively large number of equivalent nodes obtained for each concentric level confirms the fact that these two types of supposedly regular networks do actually a wide dispersion of node degrees, especially in the case of the ER configurations. That is the reason why equivalent models which do not take into account such a heterogeneity cannot yield accurate predictions.

Though the partitioning of the concentric levels in terms of groups of nodes with identical degrees was critical for proper modeling of the oscillatory dynamics, it supplied as byproduct a new hierarchical measurement corresponding to the number of nodes with specific degrees at each concentric level. Because such features have been presently found to be essential for the integrate-and-fire dynamics, it is likely that they will also provide valuable resources for the characterization of the topology of the networks.

The weights of the equivalent models obtained for each of the ER configurations are shown in Figure 12. The equivalent nodes are organized bottom-upwards along the columns and rows according to increasing degrees of the respectively subsumed original nodes. It is clear from these matrices that there are some equivalent nodes which receive converging intense weights (the clearer rows in the matrices — recall that we adopt the convention that the edges extend from the columns towards the rows). Such nodes are particularly important for the non-linear dynamics because of their greater tendency to spike, defining the main avalanches.

We now present some predictions of the dynamical features as obtained by using the respective equivalent models. Figure 13 shows the number of spikes predicted by

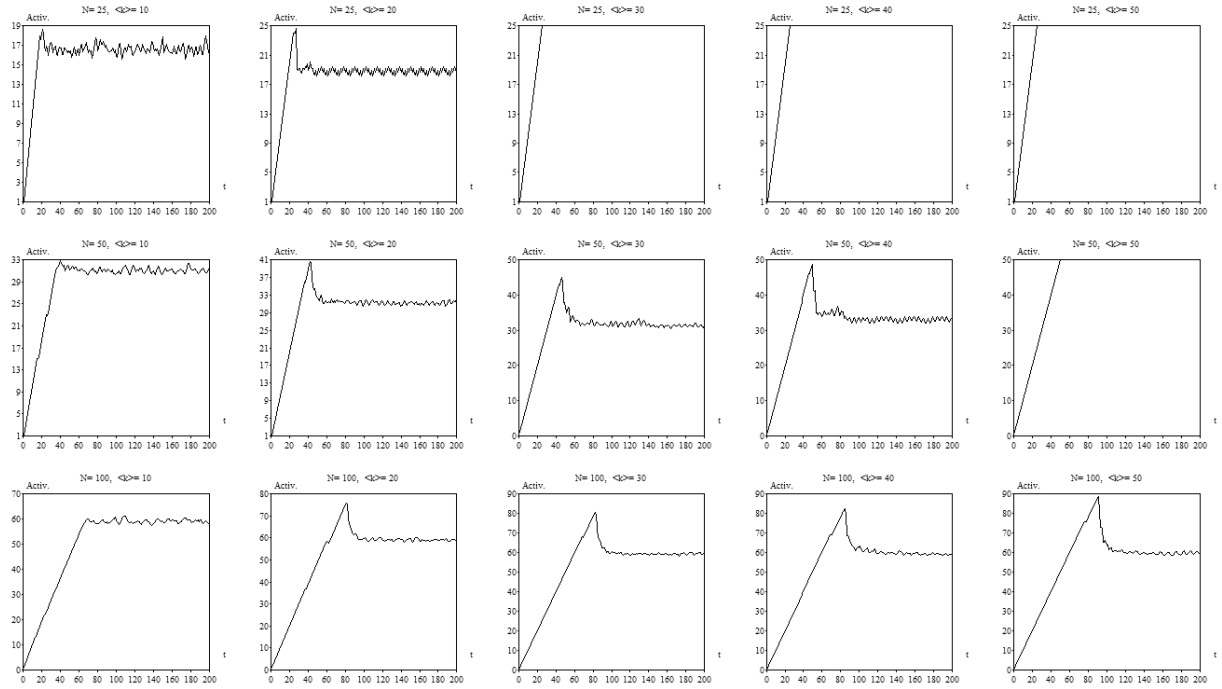

FIG. 6: The total activation inside the complex neuronal networks is not conserved (recall that activation is being continuously fed from the source node) after the main avalanche, but rather reaches a plateau of activation after the transient regime.

	$\langle k\rangle = 10$	$\langle k\rangle = 20$	$\langle k\rangle = 30$	$\langle k\rangle = 40$	$\langle k\rangle = 50$
$N = 25$	1, 17, 7	1, 23, 1	1, 24	1, 24	1, 24
	17, 72, 0	23, 23, 0	24, 0	24, 0	24, 0
	16: (1) (10) (5)	**5:** (1) (3) (1)	**2:** (1) (1)	**2:** (1) (1)	**2:** (1) (1)
$N = 50$	1, 14, 35	1, 35, 14	1, 42, 7	1, 45, 4	1, 49
	14, 168, 0	35, 310, 0	42, 246, 0	45, 176, 0	49, 0
	23: (1) (10) (12)	**22:** (1) (13) (8)	**17:** (1) (12) (4)	**9:** (1) (6) (2)	**2:** (1) (1)
$N = 100$	1, 12, 83, 4	1, 36, 63	1, 67, 32	1, 68, 31	1, 75, 24
	12, 189, 80, 0	36, 859, 0	67, 1117, 0	68, 1333, 0	75, 1358, 0
	31: (1) (9) (17) (4)	**34:** (1) (15) (18)	**33:** (1) (19) (13)	**36:** (1) (20) (15)	**34:** (1) (20) (13)

TABLE I: Features of the equivalent models obtained for the ER configurations: number of nodes per level (first line); hierarchical degrees of each level (second line); and total number of equivalent nodes (bold, third line) and the number of equivalent per concentric level (within brackets).

the equivalent model for all the considered ER configurations. By comparing with the respective real number of spikes shown in Figure 4, it becomes clear that the equivalent model allowed an impressive estimation of both the transient and steady-state dynamics in every case.

The spectra predicted for the ER configurations by using the equivalent model are shown in Figure 5. Again, an impressive similarity can be appreciated between the real values in Figure 14

Similarly impressive predictions of several aspects of the dynamics were also obtained for the WS configurations but are not shown here.

VII. OVERALL DISCUSSION

At this point, after having characterized several aspects of the integrate-and-fire dynamics obtained for the original networks, as well as the features of the respective equivalent models and predictions, it is time to integrate all such information in order to obtain a more comprehensive explanation of the origin and properties of the oscillations observed for the integrate-and-fire complex neuronal networks.

The two clusters of correlations observed for the ER model (Fig. 8) are particularly relevant, suggesting that

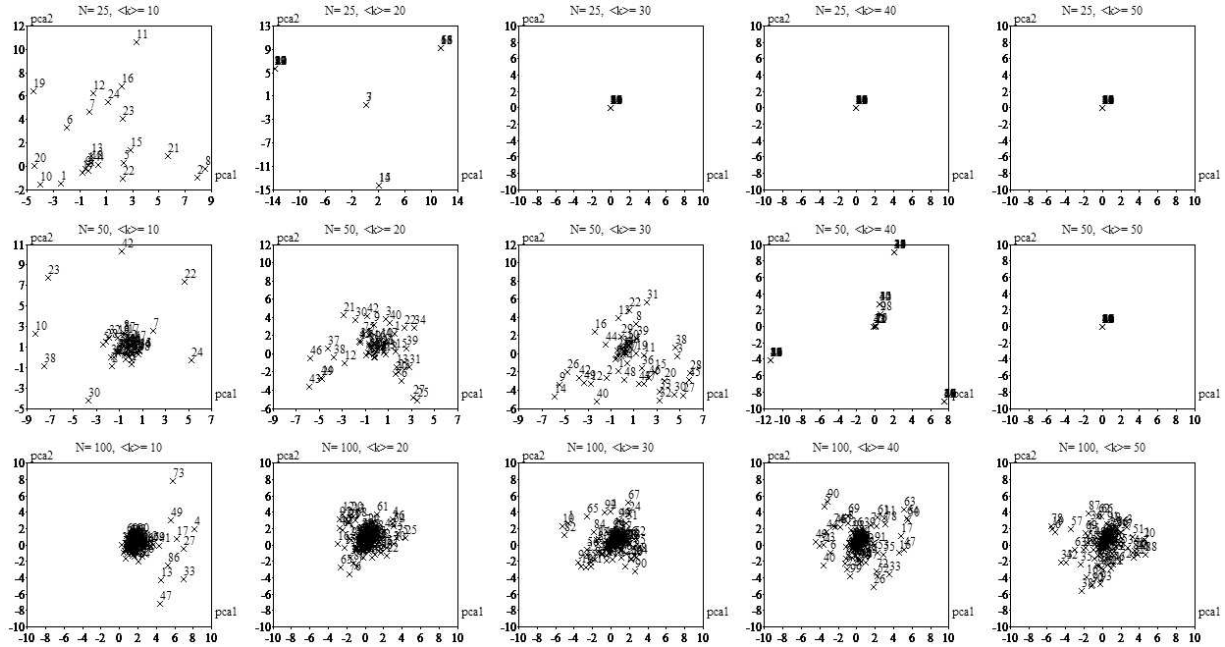

FIG. 7: The two-dimensional scatterplots obtained by the application of the PCA method over the spike patterns of each neuron in the ER configurations.

	$\langle k\rangle = 10$	$\langle k\rangle = 20$	$\langle k\rangle = 30$	$\langle k\rangle = 40$	$\langle k\rangle = 50$
$N = 25$	1, 10, 12, 2	1, 18, 6	1, 21, 3	1, 23, 1	1, 21, 3
	10, 32, 15, 0	18, 84, 0	21, 54, 0	23, 21, 0	21, 57, 0
	9: (1) (2) (4) (2)	**10:** (1) (6) (3)	**9:** (1) (5) (3)	**8:** (1) (6) (1)	**10:** (1) (6) (3)
$N = 50$	1, 9, 14, 24, 2	1, 19, 26, 4	1, 28, 21	1, 38, 11	1, 46, 3
	9, 36, 54, 17, 0	19, 131, 62, 0	28, 271, 0	38, 309, 0	46, 114, 0
	15: (1) (4) (4) (4) (2)	**17:** (1) (6) (8) (2)	**16:** (1) (8) (7)	**16:** (1) (9) (6)	**12:** (1) (8) (3)
$N = 100$	1, 11, 34, 38, 16	1, 21, 57, 21	1, 27, 55, 1	1, 42, 57	1, 50, 49
	11, 57, 118, 91, 0	21, 179, 260, 0	27, 312, 338, 0	42, 577, 0	50, 843, 0
	18: (1) (3) (4) (6) (4)	**21:** (1) (7) (9) (4	**23:** (1) (8) (9) (5)	**22:** (1) (11) (10)	**19:** (1) (9) (9)

TABLE II: Features of the equivalent models obtained for the WS configurations: number of nodes per level (first line); hierarchical degrees of each level (second line); and total number of equivalent nodes (bold, third line) and the number of equivalent per concentric level (within brackets).

the spiking frequency tends to increase linearly with the indegree of the neurons. Indeed, the higher the indegree, the more activation a neuron will receive along time, enhancing its chance of firing. Interestingly, the nodes belonging to each of the two groups straight correlations in (Fig. 8) have been found to belong to distinct respective hierarchical levels. As the neurons at different concentric levels tend to fire with different frequencies, depending on their respective number of nodes and connections, the two groups of correlations are obtained, with the intragroup straight dispersions being accounted by the above observed tendency of the spiking frequency to increase linearly with the indegrees.

Despite the clear separation of the hierarchical levels provided by the correlation diagrams in Figure 8, it is remarkable that the spiking patterns in Figure 7 failed completely to clusterize with respect to the hierarchies. This interesting fact can be taken as an indication that though the nodes belonging to different hierarchical levels do present a well-defined *mean frequency*, they are highly irregular as far as the interspike times are concerned. This can indeed be corroborated by the visual analysis of the spikegrams in Figure 3 as well as from the rich spectra (in the sense of exhibiting many frequencies) shown in Figure 5. With this respect, it would be interesting to consider PCA projections taking into account smoothed versions of the spiking patterns, which would enhance the correlations between those patterns and perhaps make

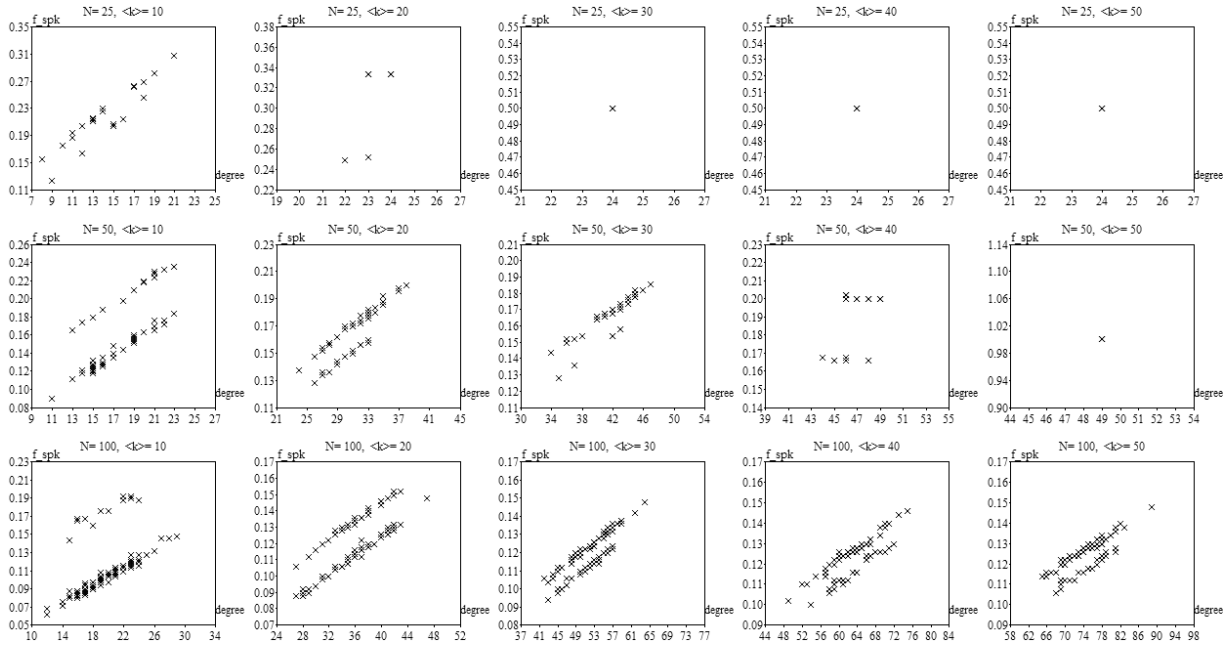

FIG. 8: The relationships between the total number of spikes per time step generated by each neuron and the respective degrees for all the considered ER configurations. The number of spikes were counted during the last 500 steps of 1000 steps-long signals.

more evident the hierarchical clusters.

Because the considered WS structures implied larger number of hierarchical levels (see Tab. II), with respective neurons firing at distinct group frequencies, the linear relationship between the spiking frequency and the indegree became blurred in the respective scatterplots in Figure 11.

VIII. CONCLUDING REMARKS

Though relatively simple, the integrate-and-fire model yields rich dynamical features, including avalanches, activation confinement inside communities and oscillations. Having addressed and explained the first two phenomena by using equivalent models [19, 20], it is now interesting to consider the origins and properties of the oscillations observed at both transient and equilibrium regimes in integrate-and-fire complex neuronal networks. This constituted precisely the objective of the present work. Its main contributions are reviewed and discussed as follows.

Characterization of Several Aspects of the Oscillations: The oscillations in the integrate-and-fire complex neuronal networks were characterized in terms of several measurements and approaches, including the visualization of the spikegrams, the total number of spikes along time and respective power spectra, total activation along time, PCA decorrelation of the spiking patterns in order to seek for clusterized dynamics features, as well as correlations between the total number of spikes and degrees of each neuron. Each of these approaches allowed interesting complementary insights about the oscillatory behavior in uniformly-random (ER) and small-world (WS) configurations. Particularly revealing were the twin correlations observed for both models, which were found to correspond to different frequencies of oscillations taking place at different concentric levels of the networks. Such correlations also indicated that the mean spiking frequency is linearly related to the indegree of the respective neurons, which constutes a particularly relevant property of the analyzed structures. Analogously to the investigation of linear diffusive dynamics reported in [32], this property links structure and oscillatory dynamics, implying that topological hubs will also become hubs of activity in the integrate-and-fire dynamics. The scatterplots obtained by the PCA projection of the individual spiking patterns yielded interesting structures which, however, were not in correspondence with the twin-correlation partitioniongs. The spectra, rich in frequencies, confirmed the complex structure of the spikings.

Identification of Two Clearly-Defined Regimes: The consideration of the total activation along time revealed two distinct and well-defined regimes: a conservative transient period, followed by the dissipative steady-state regime. The critical point separating these two dynamics was found to correspond to the main avalanches. The transient evolution was found to be more gradual for the WS configurations, which could be indeed expected because of the less pronounced (if any) avalanches in this

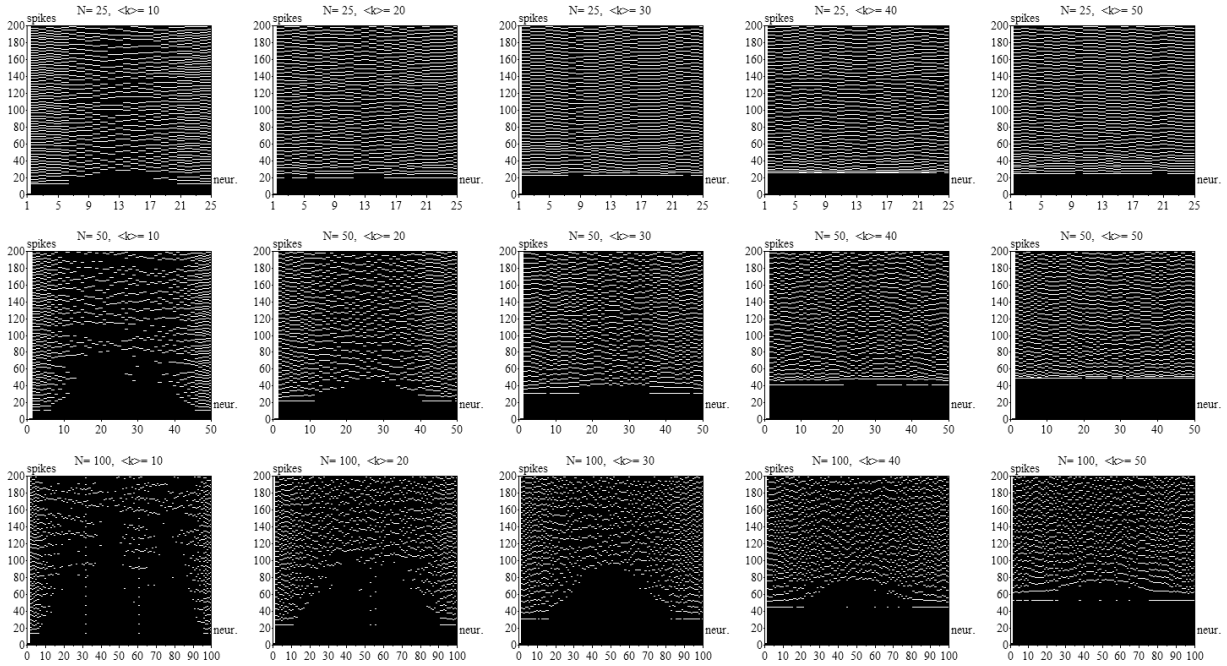

FIG. 9: The spikegrams obtained for the WS configurations.

type of networks.

Equivalent Model for Non-Uniform Degrees: Following the comprehensive characterization of the oscillatory properties of the integrate-and-fire dynamics in complex neuronal networks, an enhanced equivalent model was developed which takes into account the diversity of degrees within each concentric topological level. More specifically, the nodes with identical degrees at each of the levels are associated to respective equivalent nodes, allowing a more detailed model. Such a modification was found to be critical for paving the way to impressively accurate predictions of both the transient and steady-state features of the non-linear dynamics.

Limitation of the Stored Activation: Differently from the previous approaches reported in [16–20], the activation stored inside the state (memory) of each neuron was limited to be at most equal to the respective threshold. In addition to being more biologically-realistic in which concerns neuronal networks, this choice also allowed more interesting oscillatory dynamics.

Additional Hierarchical Measurements of Network Topology: In addition to paving the way for precise estimations of the dynamics, the enhanced equivalent model also yielded as a byproduct new hierarchical measurements corresponding to the number of nodes with specific degrees found at each of the respective concentric levels. Because such topological features proved to be fundamental for modeling the non-linear integrate-and-fire dynamics, it is expected that they can also provide valuable features for the characterization and classification of complex networks [30].

Identification of the Origin and Properties of Oscillations: As a consequence of the comprehensive characterization and modeling of the integrate-and-fire dynamics, a better understanding of the origins and properties of the spiking oscillations have been achieved. Of special importance are the positive correlations between the mean spiking frequency and the neuron indegrees and the fact that nodes at distinct concentric levels tend to fire with different ensemble frequencies. The combination of these two effects yielded the remarkable twin-correlation diagrams. In addition, it has been found that the oscillations tend to unfold after the main avalanches, i.e. along the steady-state of the dynamics, as revealed by the total activation in terms of time.

Several are the possibilities for further related investigations. In principle, most of the suggestions for future work identified in [16–20] can be immediately extended to the present work. More specific possibilities for futher investigations are identified and briefly discussed in the following.

Further Simplifications by Considering Degree Intervals: It would be interesting to consider the subsuming of the nodes in each concentric level not strictly under the condition of identical degrees, but by having similar degrees (i.e. comprised within specific intervals). Such a modification would immediately contribute to a further reduction of the overall number of equivalent nodes, making the equivalent models more compact. It would be interesting to quantify the effect of such a sim-

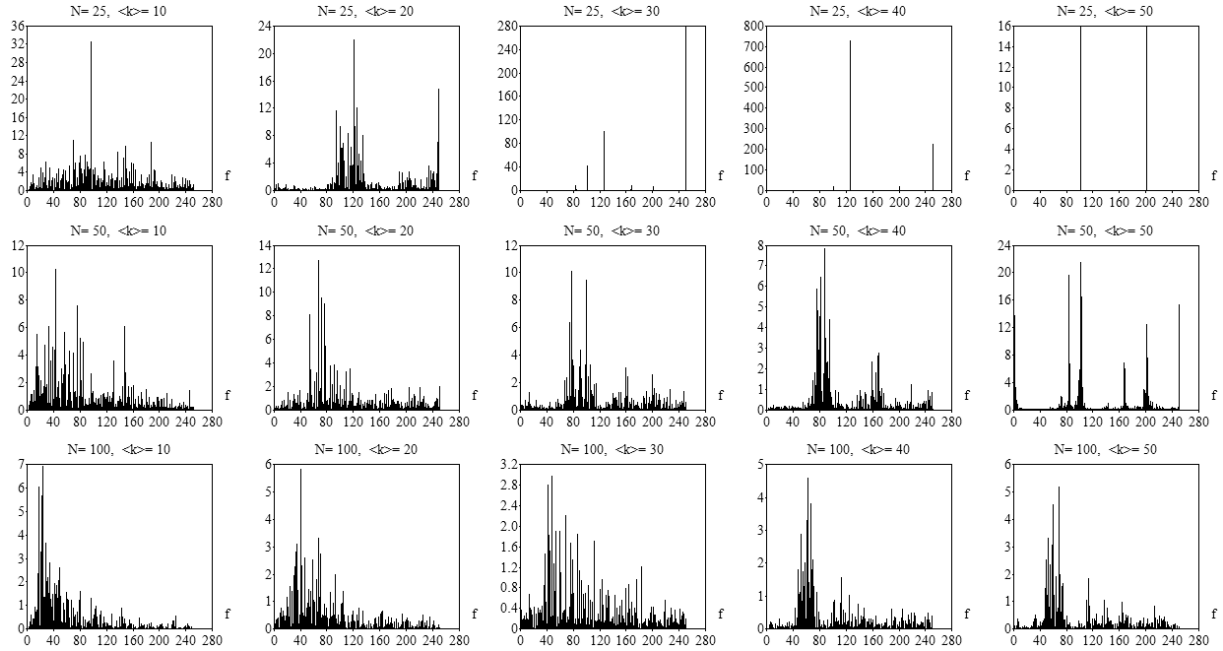

FIG. 10: The power spectra obtained for the number of spikes produced by the whole original WS networks.

plification on the accuracy of the respective predictions of the dynamical features.

Modular Equivalent Model with Non-Uniform Degrees: Because of the finer level of representation allowed by the currently reported equivalent model, it would be potentially useful to extend the previous equivalent models used to explain and predict avalanches and activation confinement inside communities.

Oscillation Analysis with Action Potentials: While the current work, analogously to the previous works [16–20], considered the activation of each spike to be equally distributed amongst the outgoing edges (i.e. axons), it would be interesting to consider the more biologically-realistic hypothesis that the spikes have constant amplitude (action potential). Preliminary investigations have already indicated that avalanches, activation confinement and oscillations are all present in this type of non-linear dynamics. However, it would be interesting to perform more systematic related investigations.

Chaos and Chaos Control: The particularly complex spiking patterns obtained after the main avalanche suggest that the dynamics of the considered networks may be chaotic. It would be particularly promising to apply methods from dynamics systems, such as delay diagrams and fractal dimensions, in order to search for chaotic behavior in the integrate-and-fire complex neuronal networks. Another interesting perspective would be to apply concepts from chaos control in order to interfere with the several remarkable aspects of the investigated dynamics.

Distinct Weights: So far, we have been limited to integrate-and-fire complex neuronal networks containing identical weights. Indeed, the weights have only been used in order to obtain the respective equivalent models. In this case, the weights correspond to the proportions of the activations (edges) which are sent to each equivalent node. It would be interesting to consider complex neuronal networks incorporating weights, in order to investigate the effects of such distributions on the respective dynamics.

Investigation of Oscillations in Other Theoretical Complex Networks Models: Because of space restrictions, the oscillatory behavior of integrate-and-fire complex neuronal networks described in this work has been restricted to a uniformly-random and a small-world theoretical models of complex networks. It would be particularly promising to extend such an investigation to other important types of network topologies, especially scale free and geographical. The consideration of the highly regular knitted structures [33] would also be interesting.

Applications to Real-World Problems: Though we have so far considered the oscillations in theoretical models of complex neuronal networks, the respective concepts and methods are immediately applicable to real-world networks. Of particular interest would be to characterize and model the neuronal network of *C. elegans*, as well as cortical networks.

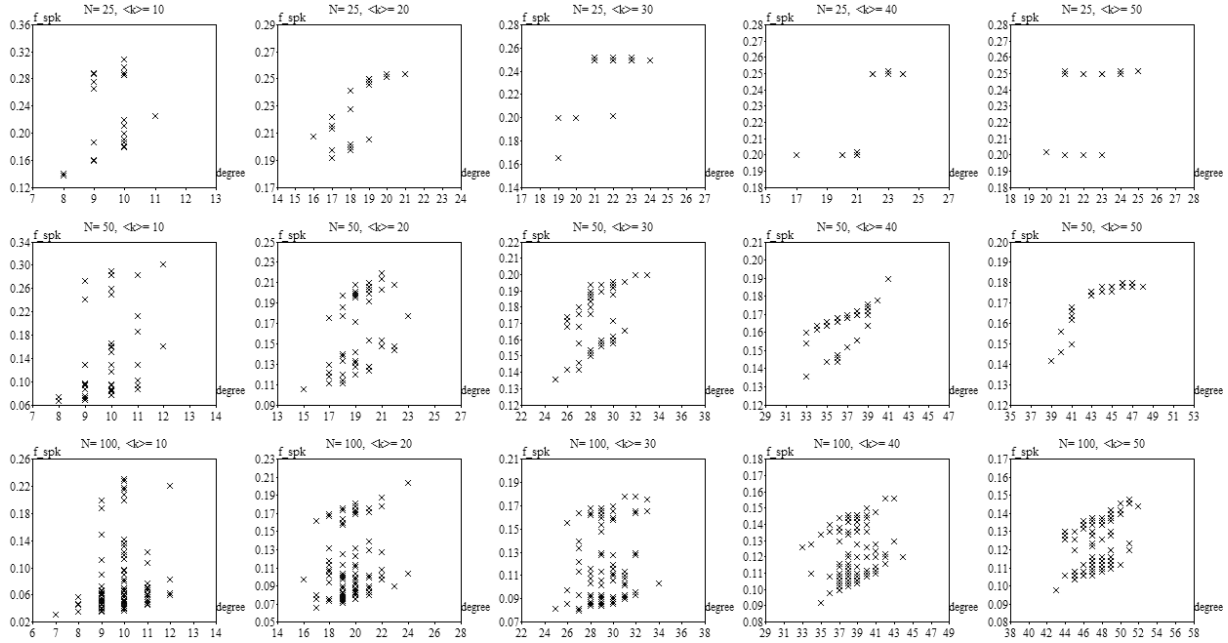

FIG. 11: The relationships between the total number of spikes per time step generated by each neuron and the respective degrees, all the considered WS configurations. The number of spikes were counted during 1000 time steps.

Acknowledgments

Luciano da F. Costa thanks CNPq (308231/03-1) and FAPESP (05/00587-5) for sponsorship.

[1] M. E. J. Newman, SIAM Rev. **45**, 167 (2003).
[2] S. Boccaletti, V. Latora, Y. Moreno, M. Chavez, and D. Hwang, Phys. Rep. **424**, 175 (2006).
[3] A. T. Bernardes, D. Stauffer, and J. Kertesz, Eur. Phys. J. B **25**, 123 (2002).
[4] L. da F. Costa, Intl. J. Mod. Phys. C **15**, 371 (2004).
[5] S. Fortunato (2004), arXiv:cond-mat/0405083.
[6] D. U. Hwang, M. Chavez, A. Amann, and S. Boccaletti, Phys. Rev. letts. **94**, 138701 (2005).
[7] C. Zhou, A. E. Motter, and J. Kurths, Phys. Rev. Letts. **96**, 034101 (2006).
[8] I. Lodato, S. Boccaletti, and V. Latora, Phys. Rev. Letts **78**, 28001 (2007).
[9] F. Sorrentino and E. Ott, Phys. Rev. E **76**, 056114 (2007).
[10] J. A. Almendral and A. D. Guilera (2007), arXiv:0705.3216.
[11] A. Aleksiejuk, J. A. Holyst, and D. Stauffer, Physica A **310**, 260 (2002).
[12] L. da F. Costa and O. Sporns, Intl. J. Bif. Chaos **17**, 2387 (2007).
[13] L. R. Squire, F. E. Bloom, S. K. McConnell, J. L. Roberts, N. S. Spitzer, and M. J. Zigmond, *Fundamental Neuroscience* (Academic Press, 2003).
[14] S. Zeki, *Inner Vision: An exploration of art and the brain* (Oxford University Press, 1999).
[15] D. H. Hubel and T. N. Wiesel, *Brain and Visual Perception* (Oxford University Press, 2005).
[16] L. da F. Costa (2008), arXiv:0801.3056.
[17] L. da F. Costa (2008), arXiv:0801.4269.
[18] L. da F. Costa (2008), arXiv:0801.4684.
[19] L. da F. Costa (2008), arXiv:0802.0421.
[20] L. da F. Costa (2008), arXiv:0802.1272.
[21] L. da F. Costa, Phys. Rev. Lett. **93**, 098702 (2004).
[22] L. da F. Costa and R. F. S. Andrade, New J. Phys. **9**, 311 (2007).
[23] L. da F. Costa and F. N. Silva, Journal of Statistical Physics **125**, 845 (2006).
[24] L. da F. Costa and L. E. C. da Rocha, The Eur. Phys. J. B **50**, 237 (2005).
[25] L. da F. Costa (2005), arXiv::cond-mat/0502156.
[26] L. da F. Costa, Phys. Rev. E **70**, 056106 (2004), cond-mat/0312712.
[27] L. da F. Costa and R. M. Cesar, *Shape Analysis and Classification: Theory and Practice* (CRC Press, 2001).
[28] G. J. McLachlan, *Discriminant Analysis and Statistical Pattern Recognition* (John Wiley and Sons, 1998).
[29] R. O. Duda, P. E. Hart, and D. G. Stork, *Pattern Clas-*

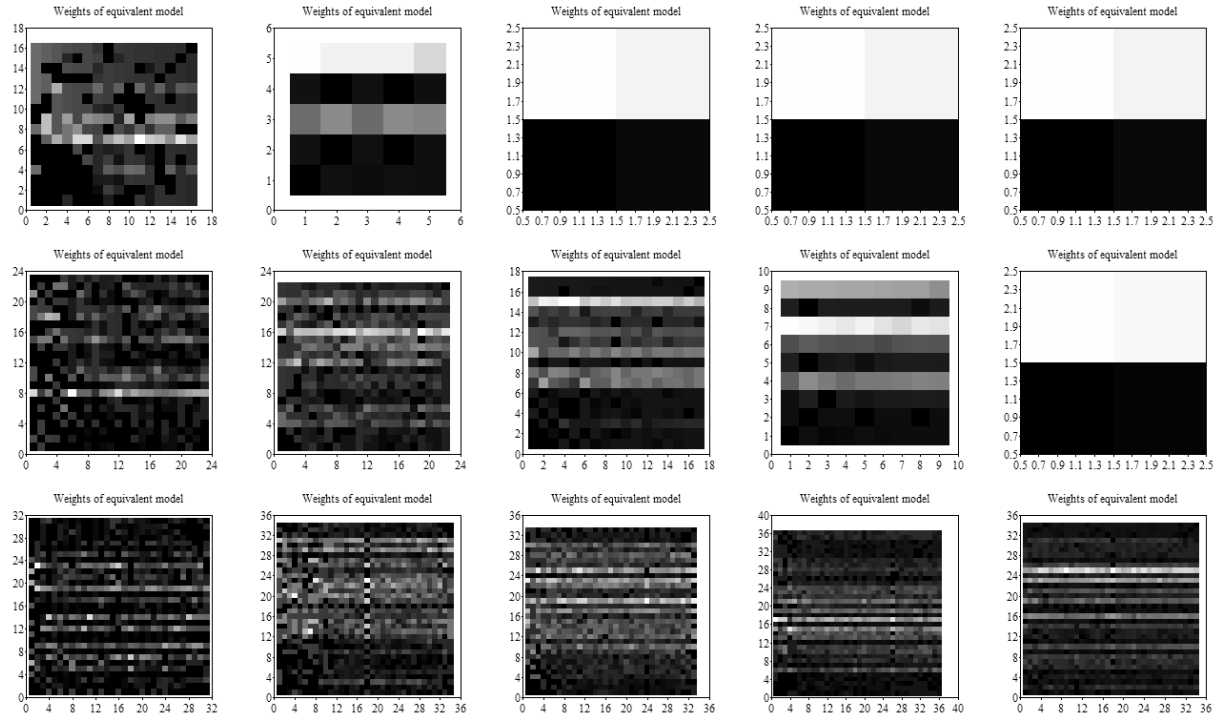

FIG. 12: The weights of each of the equivalent models obtained for the ER configurations.

sification (Wiley Interscience, 2000).
[30] L. da F. Costa, F. A. Rodrigues, G. Travieso, and P. R. V. Boas, Advs. in Phys. **56**, 167 (2007).
[31] M. A. L. Nicolelis, *Methods for Neural Ensemble Recordings* (CRC Press, 1998).
[32] L. da F. Costa, O. Sporns, L. Antiqueira, M. G. V. Nunes, and O. N. Oliveira, Appl. Phys. Letts. **91**, 054107 (2007).
[33] L. da F. Costa (2007), arXiv:0711.2736.
[34] P. J. Flory, Journal of the American Chemical Society **63**, 3083 (1941).
[35] see also [34].
[36] Though the order of the neurons in such diagrams is arbitrary, the way in which the WS networks were generated in this work tends to yield respective adjacency.

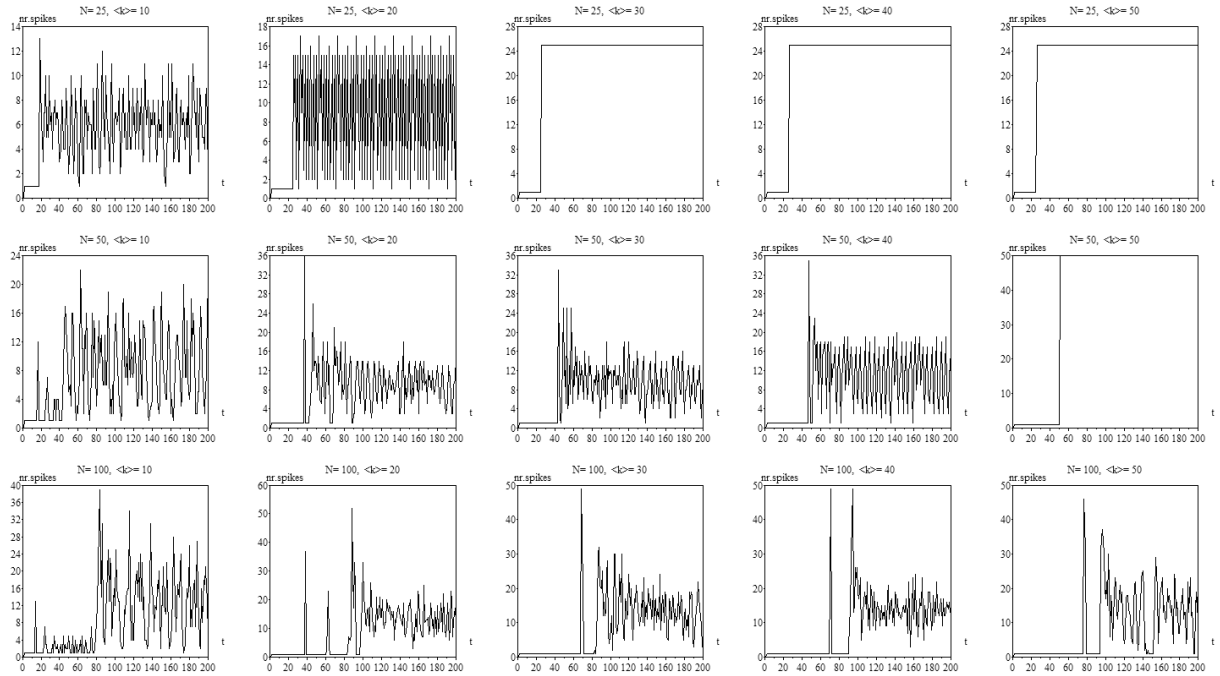

FIG. 13: The total number of spikes along time t for the ER configurations as predicted by the respective equivalent models.

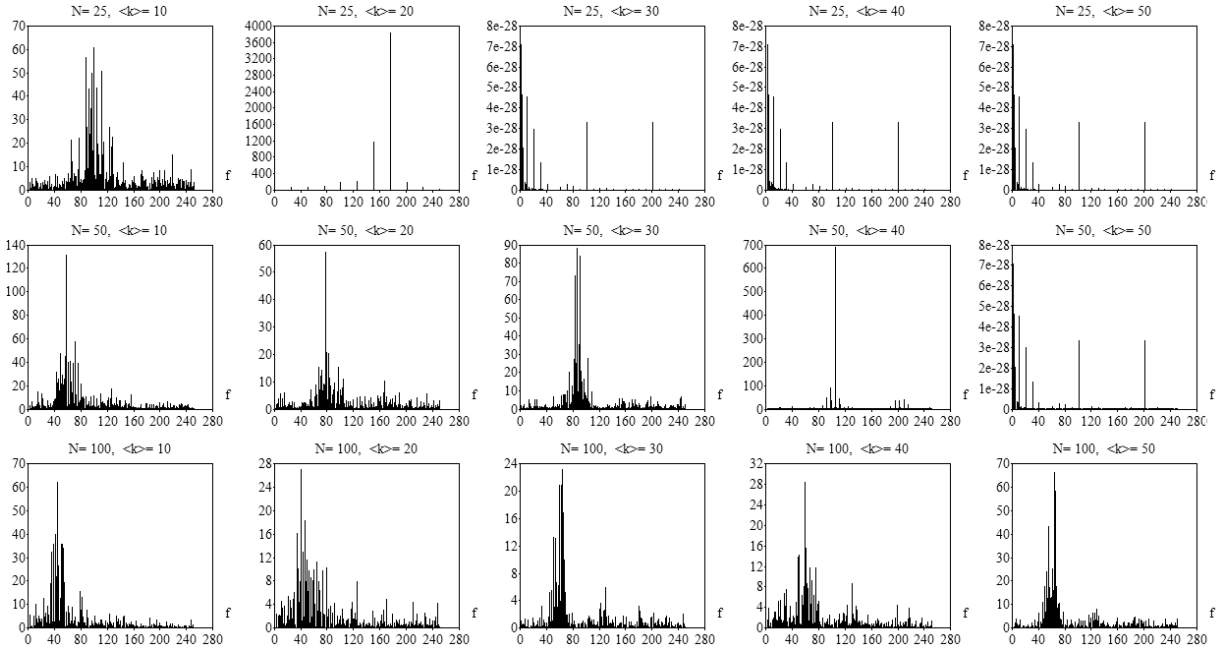

FIG. 14: The power spectra predicted by the respective equivalent models for the ER configurations.